

# Repellent Pheromones for Effective Swarm Robot Search in Unknown Environments

Filip Fossum  
CRAB lab, IDI, NTNU,  
Trondheim, Norway  
Email: filipf@stud.ntnu.no

Jean-Marc Montanier  
CRAB lab, IDI, NTNU,  
Trondheim, Norway  
Email: jean-marc.montanier@idi.ntnu.no

Pauline C. Hadow  
CRAB lab, IDI, NTNU,  
Trondheim, Norway  
Email: pauline@idi.ntnu.no

**Abstract**—In time-critical situations such as rescue missions, effective exploration is essential. Exploration of such unknown environments may be achieved through the dispersion of a swarm of robots. Recent research has turned to biology where pheromone trails provide a form of collective memory of visited areas. Rather than the attractive pheromones that have been the focus of much research, this paper considers locally distributed repellent pheromones. Further, the conditions for maximising search efficiency are investigated.

## I. INTRODUCTION

When environments are inhospitable or time is critical, autonomous robots can be deployed to assist in search and rescue operations [1]. In such situations, the purpose of the robots is to discover points of interest as efficiently as possible. As such, redundant exploration should be avoided i.e. more than one robot exploring the same area. Further, the area needs to be fully searched i.e. achieving maximum global coverage.

Approaches to achieving coverage of an environment include both *static* and *dynamic* approaches [2]. Static approaches require convergence to a static solution where a configuration of robots is achieved, ensuring that as many points in the environment as possible are within a robot's sensor range i.e. coverage is maximised. Coverage is thus the area of the environment currently observable, given the number of robots in the environment and their individual coverage. Such an approach requires that the number of robots available and their locations is sufficient so as to provide coverage for a given environment. Thus the critical number of robots required for full but efficient coverage, increases as the size or complexity of the environment increases, where complexity may be interpreted with respect to the obstacles in the environment. If the environment is unknown, then selecting such a critical number of robots can be difficult or impossible and further such a critical amount of robots may not be available. In dynamic approaches, as in the work herein, coverage of the environment is achieved due to the movement of robots around the environment and measured over a period of time. Efficient solutions need to minimise the overlapping movements of the robots i.e. overlapping exploration paths; whilst ensuring maximum coverage in the minimum time.

Inspiration to meet the efficient search challenge may be taken from the indirect communication of social insects: pheromones. Pheromones are chemical compounds that may be released and observed by the individuals of a swarm. When an ant finds food, it releases its pheromone on its

way home and thus leaves a pheromone trail. Other ants can follow this trail and amplify it with their own pheromone to attract even more ants [3]. Such a pheromone trail is termed an attractive pheromone and has received much attention in swarm robotics. In [4]–[6] attractive pheromones have been investigated, incorporating a central server storing pheromone data.

To avoid centralised storage, local pheromone solutions have been proposed [7], [8]. In both works, virtual pheromones are transmitted through infra-red emitters and receivers in a relay type fashion. At each transmission, the virtual pheromone is modified e.g. a hop counter associated to the pheromone is decreased. The gradient of the virtual pheromone is then computed locally by each based on all messages received. Within this approach the precision of the gradient is dependent of the number of robots involved and the number of messages exchanged. Alternatively, the use of chemicals to represent pheromones has been studied in [9], intended for environments where inter-robot radio communication is either infeasible or undesirable. In the tasks challenged by local pheromones solution the robots should reach one specific area, which leaves the problem of rapid dispersion in the environment as unaddressed.

In biology, a further solution is repellent pheromones. In [10], such repellent pheromones were released during exploration, maximising the distance between robots so as to enforce an even distribution of robots in the environment. Thus a static solution was sought, again requiring a critical number of robots for a given environment. In [11] a dynamic solution was investigated, reducing the critical number of robots required. However, the repellent pheromone data was stored in internal maps that were distributed globally between all robots, again raising the global communication challenge and its inherent scalability issues. Moreover, the effect of the size of the environment and the number of robots on the performance of this approach were not investigated.

In this work, a dynamic approach to repellent pheromones is proposed. Further, the efficiency of the approach is investigated with respect to different environments and available number of robots. Further, the affect of the evaporation rate of the pheromones is investigated. Section II provides details on the robot architecture, followed by details on the pheromone model used in section III. In section IV the experimental setup is presented, followed by the results obtained. Finally, the conclusion and discussions for further work are presented in section VI.

## II. ROBOT IMPLEMENTATION

The simulated robot architecture applied in this work is based on the ChIRP robot [12], extended with 4 pheromone sensors and is simulated using the Roborobo! robotic simulator [13]. Each robot has a round body, 5 pixels in diameter and can move at a maximum velocity of  $1 \text{ pixel}/\text{timestep}$ . 2 actuators are connected to the wheels. By slowing down either actuator the robot will turn in the corresponding direction at an angle proportional to the difference in actuator speeds. There are eight evenly distributed proximity sensors as well as 4 pheromone sensors — see figure 1. Each proximity sensor has a range of 30 pixels, thus able to measure the distance to obstacles within this range. Each pheromone sensor is positioned 20 pixels from the robot center and measures the intensity of pheromone directly beneath it.

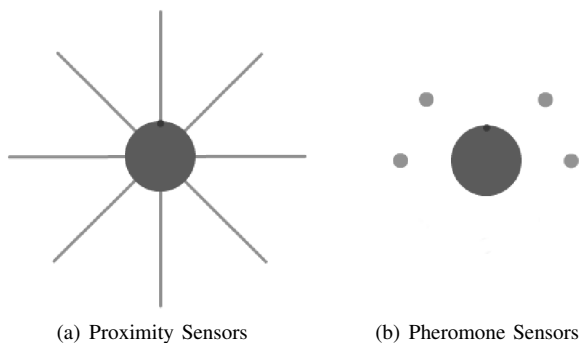


Fig. 1: Sensor placement of robots

The architecture of the controller is based on Brooks' subsumption architecture [14], as shown in figure 2.

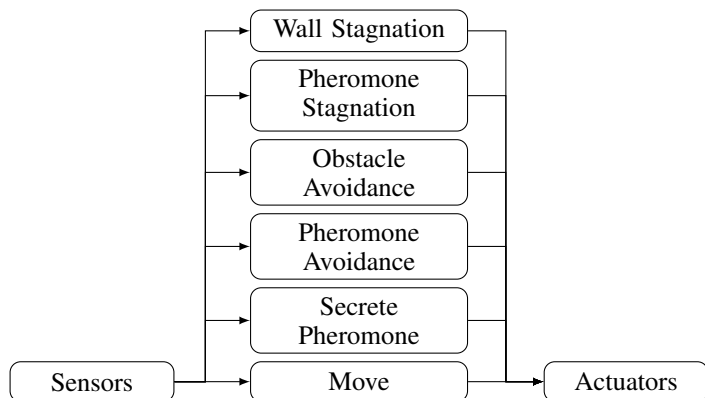


Fig. 2: Robot controller architecture

The pheromone avoidance layer implements the repellent pheromone process. At any given time, arbitration of the four pheromone sensor signals, selects the sensor with the highest reading. If either sensor on one side of the robot has a higher reading than the sensors on the other side, a signal is sent to the connected actuator, dampening the speed proportional to the concentration. The higher the concentration the more abrupt the turn. Otherwise the robot continues in its current direction.

As shown in figure 2, obstacle avoidance (walls, other

robots) is prioritised over pheromone avoidance. 2 proximity sensors on each side (total of four) are coupled to an actuator providing inhibitory signals i.e. a stronger signal translates to a reduction in speed of the actuator. The front sensor connects to both actuators, ensuring that the robot slows down when approaching obstacles head-on.

A further priority is that of pheromone stagnation. Since robots are continuously secreting pheromones, when such secretion is not suppressed, then the robots are highly susceptible to their own trail. Figure 3 depicts a situation where a robot is caught in a spiral of its own pheromone trail.

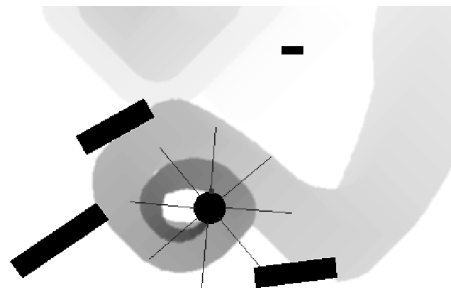


Fig. 3: Robots can become temporarily trapped by their own pheromone trail

To prevent such a situation, the pheromone stagnation level employs two counters — one for left movements and one for right movement, both initialised to 0. These counters are incremented to reflect the changes in movements caused by the pheromones concentration. However, when no change in direction is enforced by the pheromone avoidance layer, the corresponding counter decrements. Whenever one of the counters is greater than a *Rotation Threshold*, pheromone avoidance is suppressed for a period of time (termed *Pheromone Inhibition*).

Wall stagnation, on the other hand, is detected based on the robot's lack of movement in the environment. Throughout the simulation Cartesian coordinates of the robot's positions are recorded. Only the ones within a time window are conserved. The length of this window is termed *Stagnation Observation*. Standard deviation of the  $x$  and  $y$  values are calculated respectively and if less than a *Stagnation Threshold* then the robot is considered in stagnation. Stagnation resolution is carried out in two steps. The first step is to reverse for a short duration. Next, the robot will stop and rotate to face the direction with the least obstruction. This direction is decided by querying each distance sensor along with its two adjacent sensors. The collection of sensors that yields the lowest accumulated distance value determines the most desirable orientation. When the robot has rotated to face the correct direction, control is restored to the other layers.

## III. REPELLENT PHEROMONES

The pheromones are modelled as a cellular automaton [15]. The cellular space of the pheromone model is defined as a two-dimensional grid where every cell corresponds to one pixel of the environment. Each cell may take values from the range  $[0 - 255]$  which represents the pheromone intensity level of that cell. A cell with a value of 0 is in its quiescent state. Robots secrete pheromones by setting the value of a single cell,

directly beneath it, to 255. Visually the transparency channel of each pixel is directly mapped to the potency of the pheromone. A pixel with an alpha value of 255 is completely opaque, while a pixel with an alpha value of 0 is fully transparent. Figure 4 illustrates the visual movement of a robot, given this pheromone model. As shown, the pheromone path closest to the robot is the most opaque (darkest) and the furthest part of the path shown is almost transparent (lightest). The path transition from dark to light (representing the pheromones potency) is controlled by an evaporation factor whereas the breadth of the path from narrow, close to the robot to wider, further from the robot, is controlled by diffusion.

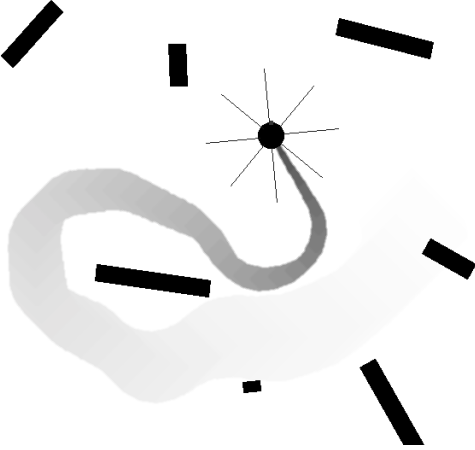


Fig. 4: Illustration of the pheromone model

The evaporation factor, given in (1) is inspired by the work of [4] for attractive pheromones. The two key parameters are the number of time steps between every pheromone update,  $\Delta t$ , and a constant  $t_c$  which determines the time allocated for the pheromone to evaporate completely.

$$\text{Evaporation Factor} = \exp\left(\frac{\log(\frac{1}{2})}{t_c} \Delta t\right) \quad (1)$$

As the pheromone model uses a Von Neumann neighbourhood, pheromones will diffuse by one pixel in each of the four cardinal directions every time step, as shown in the transition rule of figure 5. Diffusion can be controlled by modifying the pheromone update interval  $\Delta t$ . Lower values of  $\Delta t$  will cause the pheromone intensity to be updated more frequently, affecting the evaporation factor which further affects the pheromone update to every cell in the neighbourhood, given by the transition rule. Further, an averaging filter is applied to smooth out rough edges produced by the transition rule. The averaging filter is applied after the transition rule to all cells across the CA space. The pheromone value of each cell is adjusted to reflect the average value of each cell in its eight surrounding neighbours.

#### IV. EXPERIMENTAL SETUP

Table I provides an overview of the parameters applied for the experiments herein. The experiments are conducted as pairs of experiments, with or without repellent pheromones. Each such experiment pair are initialised with the same initial

$$\begin{aligned} \text{pheromone}[x][y] = & \max(\text{cell}[x+1][y], \\ & \text{cell}[x-1][y], \\ & \text{cell}[x][y+1], \\ & \text{cell}[x][y-1]) \\ & * \text{Evaporation Factor} \end{aligned}$$

Fig. 5: Transition rule of cellular automata pheromone model

Parameter	Value
Rotation Threshold	50 time steps
Pheromone Inhibition	10 time steps
Stagnation Observation	100 time steps
Stagnation Threshold	10
$\Delta t$	25 time step
Slow evaporation rate ( $t_c$ )	2000 time steps
Fast evaporation rate ( $t_c$ )	250 time steps

TABLE I: Parameters for experiments.

positions and rotations (generated randomly for the experiment pair). Further, despite the experiments being based on a physically available robot, ChIRP robot [12], a simulation environment was chosen for these initial experiments. The possibility to transfer this work to the physical robots is discussed in section VI.

As stated, the goal of this work is to maximise the coverage achieved where coverage measures how much of the environment has been visited collectively by the robots, over time. Whenever a robot is within the bounds of a tile, that tile is marked as visited. The coverage at any given time step of the simulation is the total number of tiles that are marked as visited. Coverage is thus measured as shown in equations 2. The number of tiles that need to be visited in order to achieve full coverage, naturally depends on the size of the environment. The environments applied herein vary in size between  $1000 \times 1000$  and  $2000 \times 2000$ . Since all experiments are performed with a tile size of  $50 \times 50$ , maximum coverage of these environments will be achieved at 400 and 1600 tiles covered, respectively.

$$\text{Coverage} = \frac{\# \text{Tiles Visited}}{\# \text{Total Tiles}} \quad (2)$$

As stated, it was chosen to present two unknown environments to the robots: a smaller environment with few obstacles and a larger environment with many obstacles. The environments applied and their setup parameters are illustrated in figure 8. A key issue in the generation of these environments was to ensure that there was no bias introduced i.e. providing obstacles that are less or more challenging. The algorithm applied was inspired by an algorithm for modelling street patterns [16]. Rather than creating an interconnected network of roads, as in the original algorithm, the principles were applied to generate obstacles composed of multiple line segments.

The first step of the revised algorithm is to initiate a set amount of *points* at random positions throughout the

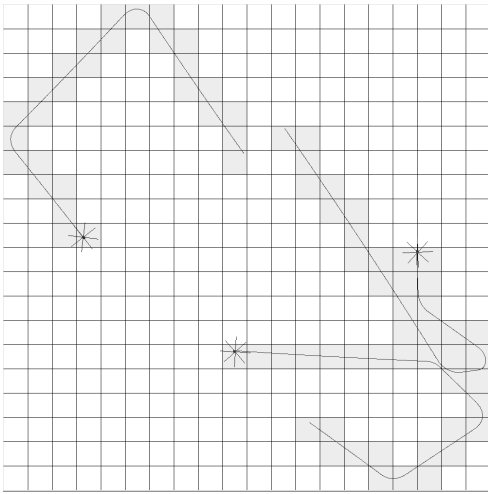
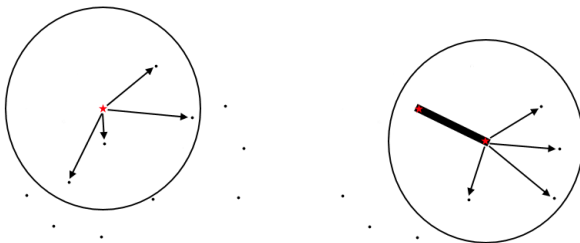


Fig. 6: Graphical representation of coverage. Highlighted tiles are covered

environment. A given number of these points will be marked as *seed points* and the remainder labelled as *regular points*, where the number of *seed points* is a user specified variable. For every seed point, vectors are drawn to all regular points within a specified *radius*, as depicted in figure 7(a). These points are removed and the average of these vectors constitute a line that acts as an obstacle in the environment (in bold in figure 7(b)), starting where the seed point was given and ending in the furthest regular point. At the end position of the newly created obstacle (line) an additional seed point is spawned. This seed point is then treated similarly to the one before, extending the obstacle (line). The maximum number of times the line will be extended is determined by a random number in the range  $[1, maxJumps]$ , where *maxJumps* is a user specified variable. If this threshold is exceeded or no points are detected within range of the specified search radius, the process is repeated for the next seed point among those initially spawned until all spawned seed points result in obstacles.



(a) Vectors are drawn from a seed point to all points within the threshold radius  
 (b) These points are deleted and the average vector form an obstacle as well as a new seed point. This repeats until no points are in range.

Fig. 7: Random environment generator

Parameter	Value
Height	1000
Width	1000
Points	500
Seeds	20
SearchRadius	300
maxJumps	5

(a) Small environment

Parameter	Value
Height	2000
Width	2000
Points	5000
Seeds	50
SearchRadius	150
maxJumps	50

(b) Large environment

Fig. 8: Environments used in experiments

## V. RESULTS

The experiments performed investigate the viability of the introduction of repellent pheromones to improve collective exploration in unknown environments. Further, the efficiency of this technique is investigated in the light of the density of robots required and the evaporation factor applied. The parameters applied in these experiments are described in table I.

### A. Repellent Pheromones with a slow evaporation rate

A small environment (see figure 8) was applied in the initial investigation to see whether repellent pheromones provided improved coverage compared to the coverage achieved without pheromones. Figure 9 depicts the difference in coverage achieved, where 40 runs were performed with 3 robots and a slow environment rate. The non-dotted lines depict the results obtained without pheromones and the dotted lines, with pheromones. The center lines represents the average coverage and the lines above and below represent the standard deviation.

The initial coverage exhibited in both cases is the same. This is to be expected — their initial locations are the same and when no pheromones are being detected, their behaviours are the same. Since practically any movement at the start of a run leads to the exploration of a new tile, the coverage increases very rapidly. As tiles start to be re-visited, the increase in coverage slows and deviation increases. This larger deviation is due to the relative location of objects and starting locations of the robots in the individual runs and the effect thereof on the movement of the robots. Further, some robots may be initialised at locations of close proximity, causing them to retrace covered ground. In the case of the pheromones, as the experiments continue the pheromones diffuse throughout

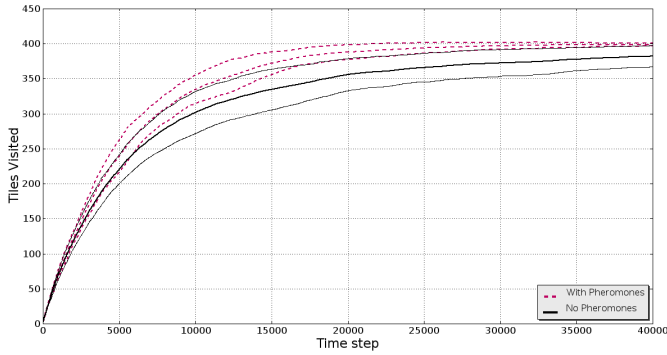


Fig. 9: Coverage: small environment, 3 robots and slow evaporation rate

the environment and counteract this challenge, as shown — maximum coverage of 400 tiles is achieved at 35,000 steps.

The presence of pheromones in the environment provides dynamic influences on the robots, making them more likely to reach the final unexplored areas. To study such behaviour, figure 10 provides a trace of the movement of the robots from a single run in each of the 2 cases investigated.

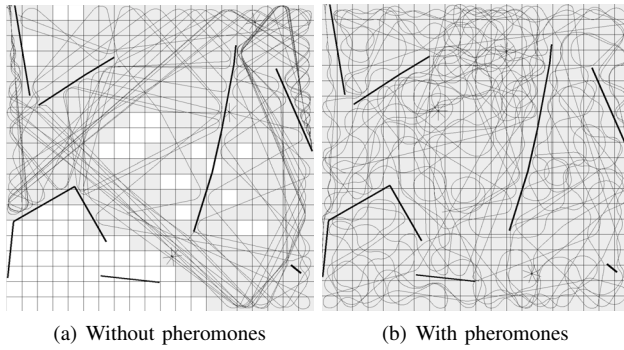


Fig. 10: Movement traces and covered tiles: small environment, 3 robots and slow evaporation rate)

Figure 10(a) shows that when pheromones are not being used, the robots may have difficulty exploring certain areas. None of the tiles in the bottom left corner are covered. In a given run, a robot may start within this region, causing the tiles within to be covered effortlessly. However, in other cases these locations can be difficult to reach, as shown. Thus as described, coverage of the environment may be highly inconsistent between runs. Figure 10(b) depicts the same simulation setup including robot initial locations, but with the inclusion of pheromones. The robots can be seen to achieve complete coverage. The pheromones enable the robots to reach all areas of the environment irrespective of their starting position. While many tiles are still covered multiple times, the coverage of the environment becomes much more even and thus may be considered as a more efficient coverage.

### B. Density of Robots

To consider the effect of an increased density of robots, the experiment of section V-A was repeated with 24 robots, as

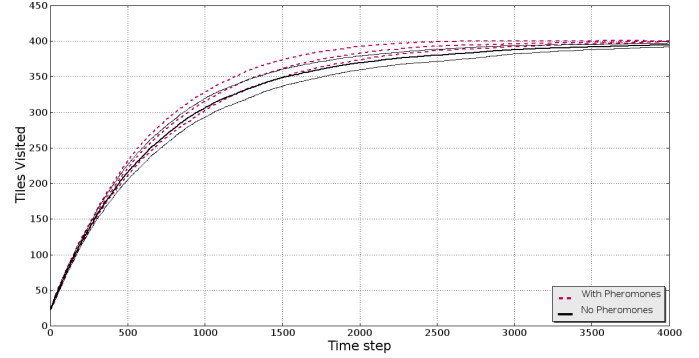


Fig. 11: Coverage: small environment, 24 robots and slow evaporation rate

illustrated in figure 11. While there is still a small advantage in coverage when using pheromones, it is apparent that the benefit decreases as the number of robots increase, for such a small environment. Complete coverage is achieved after just 4,000 time steps, irrespective of whether pheromones are applied or not. It is clear that the large number of robots provide a redundancy that all but cancel the positive effect of the introduced pheromones. With a sufficient number of robots, then the issue of location of the individual robots, discussed in section V-A, is all but removed. There is a sufficient number of robots such that some robots will be initialised in such difficult areas, each time. Thus the pheromones which support movement to difficult areas become redundant.

These results raise the question of what will happen when the environment enables significant breathing room for the robots to be further influenced by the pheromones. Once again using pheromones with a slow evaporation rate, figure 12 shows the coverage exhibited by 3 robots in an environment four times the size of the former experiments — see figure 8(b).

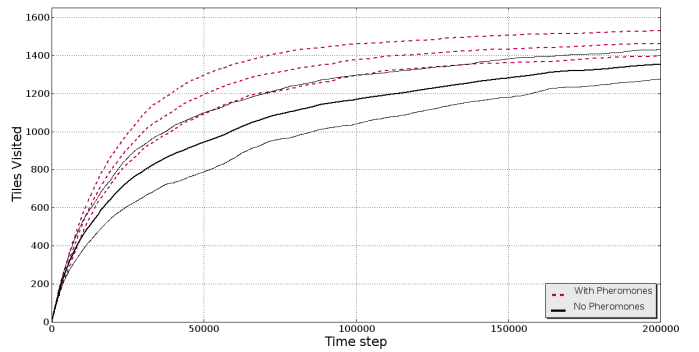


Fig. 12: Coverage: large environment, 3 robots and slow evaporation rate

Due to the vast size of the environment and the few robots applied, the maximum coverage of 1600 tiles was not reached in either case. However, the advantage of the repellent pheromones is clear and exceeds that seen in the experiments in the small environment. After 50,000 time steps, where pheromones are applied, the robots have covered an

average of 1194 tiles. This accounts for approximately 75% of the environment. On the other hand, the robots without pheromones have covered an average of 944 tiles, or 59% of the environment. After 200,000 time steps the simulations are terminated. At this point, the robots have achieved an average coverage of approximately 91% when pheromones are applied and 84% without pheromones. Since the distances in the environment are so large, a turn towards a previously explored location will negatively affect the overall coverage to a much higher degree than before.

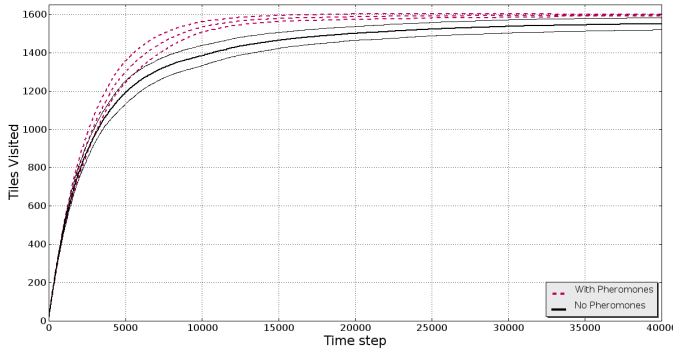


Fig. 13: Coverage: large environment, 24 robots and slow evaporation rate.

Again, the number of robots were increased, this time for the large environment — see figure 13. As expected, the difference in coverage is indeed diminished. However, after 10,000 time steps there is still a noticeable difference in coverage. At this stage, robots using pheromones have covered an average of 1533 tiles, or approximately 96% of the environment. At the same time, robots without pheromones, have covered an average of 1388 tiles i.e. approximately 87% of the environment. Recall that when 24 robots were deployed in the smaller environment (figure 11), complete coverage was achieved by both types of robot after only 4,000 time steps. In this larger environment, the coverage exhibited by the two types of robots does not start to converge towards the optimal until after 40,000 time steps, where the robots with pheromones have reached almost complete coverage already at 15000 time steps. However, maximum coverage is not achieved, in the absence of pheromones.

Since the measure of coverage makes no distinction between the various tiles of the environment, it is difficult to determine why maximum coverage is not achieved without pheromones in this case. In order to get a non-binary representation of how tiles are covered across a collection of simulations, heat maps were created to highlight which tiles of the environment the robots are more frequently revisiting. The heat maps were created by keeping individual counters for each tile. Whenever a robot is within the bounds of a tile, its counter increments. These values are normalized over the global minimum and maximum, before each tile is coloured from light to dark according to the increasing time spent in each tile. The heat map of the simulation with 24 robots in the large environment is depicted in figure 14.

It is apparent that when there is no additional guidance provided by pheromones and thus the obstacles have a stronger

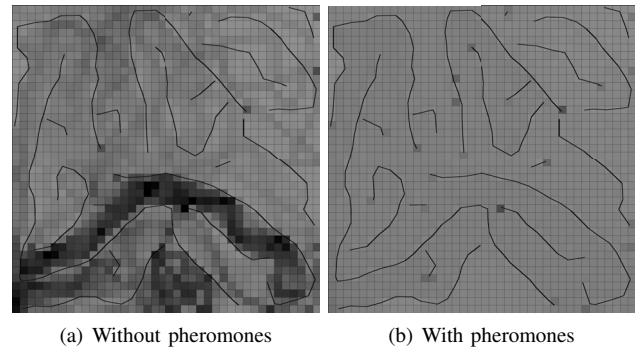


Fig. 14: Heat maps: large environment with 24 robots

effect on their movement, robots can lock themselves into repeated patterns of movement, as shown by the significant patches of darker tiles in the lower part of figure 14. When using pheromones the redundant coverage of tiles reduces significantly — note the lighter tiles of the similar area.

### C. Effect of Evaporation

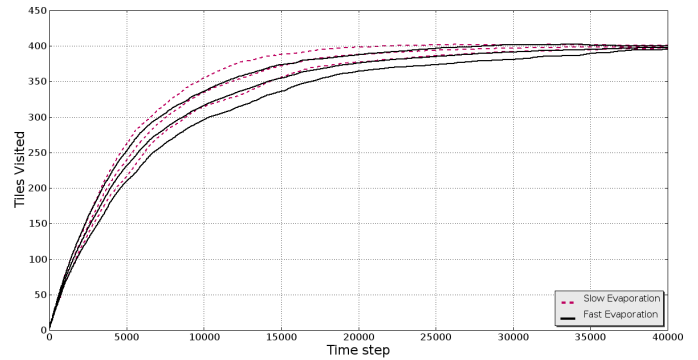


Fig. 15: Evaporation Rate effect on Coverage: small environment, 3 robots with pheromones

Changing the evaporation rate ( $t_c$ ) affects the evaporation factor and thus the updated pheromone intensity of each tile. The effect of a faster evaporation rate was investigated, as shown in figure 15. The results show that the faster evaporation rate does not improve coverage. Maximum coverage is achieved faster with a slow evaporation rate where the pheromones diffuse further before evaporating completely. Thus the effect of the pheromones secreted are more far reaching which would seem to be beneficial when few robots are covering the environment.

Increasing the number of robots in the environment provides a different picture of evaporation rates, as shown in figure 16. Here it is clear that the previous advantage of the slow evaporation rate is lost when 24 robots are moving in the environment. The far reaching effect of the longer pheromone trail has less of an advantage when more robots move around the area. As such, the longer pheromone trail may be regarded as an excess of pheromones in the environment i.e beyond that which is needed. However, as shown, these longer trails have not disadvantaged the results in this case.

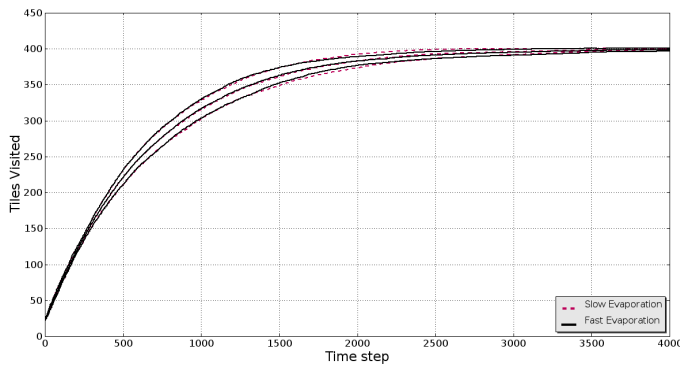


Fig. 16: Evaporation rate effect on Coverage: small environment, 24 robots with pheromones

Slow evaporation rates can, however, provide a worst case scenario where the pheromones no longer effect robot movement. As stated, the longer trail can leave an excess of pheromones in the environment. In the worst case, this excess is such that the pheromone intensity in the tiles of the environment will all be around maximum. Thus the pheromones no longer provide cues to the robots that support distribution. Thus although the pheromones are in use, the robots have to operate as wall avoidance robots i.e. the case of no pheromones.

To limit the effect of such a situation, a pheromone stagnation mechanism was implemented which exploits the fact that close to any robot, where maximum phenotype potency is secreted, there is also a faster decay, due to the logarithmic nature of the decay process. Thus even when the tiles are covered by high phenotype intensity there are still variations close to any robot.

These results show that the setting of evaporation rates is a key to achieving the advantage as well as maximising the advantage that a slower evaporation rate can achieve. Further, that such an evaporation rate choice needs to take into account the relative number of robots with respect to the area of the environment. However, the effect of evaporation is not only based on the secretion of the pheromones but also on the controller's interpretation of such values and thus the controller itself should be designed carefully so as ensure maximum coverage. One such example is the incorporation of pheromone stagnation solutions.

## VI. CONCLUSION AND DISCUSSION

The work herein presents an implementation of repellent pheromones for the exploration of unknown environments for a swarm of robots. The implementation proposed focuses on the use of local information and the viability of the approach has been studied along with the conditions in which it is beneficial.

The experiments performed show that the inclusion of repellent pheromones can indeed reduce the redundancy in search. When robots are basing their movement almost entirely on static obstacles, the location of these obstacles dictate how the robots will move. In some cases the robots can be forced to continuously retrace their own steps. Pheromones add a dynamic influence to the movement of the robots that makes them less dependent on the structure of the environment.

Ultimately, the inclusion of pheromones does not only increase the speed at which the environment is covered, but also enables exploration of areas that could otherwise be unreachable. Results showed a decrease in the advantage of pheromones as the density of robots increased. On the other hand, the results indicated that the addition of pheromones enabled fewer robots to cover the same area or in some cases, enabled a coverage that was otherwise not possible, without pheromones.

The experiments also showed a consistent improvement in coverage as the rate of evaporation was reduced. Since pheromones are only perceived locally they will inherently have no effect until robots uncover them. If pheromones evaporate too quickly they will only be able to affect those robots in a closer vicinity. Additionally, their ability to discourage robots from revisiting the same areas will be limited.

Future research is envisioned along two main axes: improving the efficiency of the model and applying the model to real robots. While the pheromones shows signs of improvement, the rate at which the environment is covered is not optimal. Situations can arise where the pheromones actually counteract the advancement of the swarm. Due to diffusion and evaporation such delays in the system are only temporary. Regardless, time is still wasted. Investigation is needed into mitigating these effects so as to further improve efficiency.

An obvious limitation of pheromones is the difficulty in representing them for physical robots. The robot controller relies on sensors that are currently 20 pixels distant from the main robot centre. Such a feature is certainly has limited feasibility in the real world. Further, the robot controller of this study relies heavily on differences in intensity values. These variations are created by the transition rule followed by the average filter applied to the pheromones. Since this operation is delimited by walls, it effectively creates gradients toward open areas and locations not recently visited by other robots. Achieving this effect in a real world setting could be a challenge. Furthermore, the variations created by the average filter are often very small. Outside of controlled environments where sensors are susceptible to noise, reliably detecting similarly small variations can be a difficult task.

## ACKNOWLEDGMENT

The authors would like to thank Christian Berg Skjetne for his technical assistance.

## REFERENCES

- [1] J. G. Blich, "Artificial intelligence technologies for robot assisted urban search and rescue," *Expert Systems with Applications*, vol. 11, no. 2, pp. 109 – 124, 1996, army Applications of Artificial Intelligence.
- [2] M. Batalin and G. Sukhatme, "Coverage, exploration, and deployment by a mobile robot and communication network," in *Information Processing in Sensor Networks*, ser. Lecture Notes in Computer Science, F. Zhao and L. Guibas, Eds. Springer Berlin Heidelberg, 2003, vol. 2634, pp. 376–391.
- [3] S. Garnier, J. Gautrais, and G. Theraulaz, "The biological principles of swarm intelligence," *Swarm Intelligence*, vol. 1, no. 1, pp. 3–31, Jun. 2007.
- [4] S. Garnier, F. Tache, M. Combe, A. Grimal, and G. Theraulaz, "Alice in pheromone land: An experimental setup for the study of ant-like robots," in *IEEE Swarm Intelligence Symposium, 2007. SIS 2007*, 2007, pp. 37–44, 00038.

- [5] O. Simonin, T. Huraux, and F. Charpillet, "Interactive surface for bio-inspired robotics, re-examining foraging models," in *Tools with Artificial Intelligence (ICTAI), 2011 23rd IEEE International Conference on*. IEEE, 2011, pp. 361–368.
- [6] A. Filipescu, I. Susnea, S. Filipescu, and G. Stamatescu, "Wheeled mobile robot control using virtual pheromones and neural networks," in *IEEE International Conference on Control and Automation, 2009. ICCA 2009*, 2009, pp. 157–162, 00000.
- [7] D. Payton, R. Estkowski, and M. Howard, "Pheromone robotics and the logic of virtual pheromones," in *Swarm Robotics*, ser. Lecture Notes in Computer Science, E. Sahin and W. M. Spears, Eds. Springer Berlin Heidelberg, Jan. 2005, no. 3342, pp. 45–57.
- [8] T. Schmickl and K. Crailsheim, "Trophallaxis among swarm-robots: A biologically inspired strategy for swarm robotics," in *The First IEEE/RAS-EMBS International Conference on Biomedical Robotics and Biomechatronics, 2006. BioRob 2006*, 2006, pp. 377–382.
- [9] A. H. Purnamadajaja and R. A. Russell, "Guiding robots behaviors using pheromone communication," *Autonomous Robots*, vol. 23, no. 2, pp. 113–130, Aug. 2007.
- [10] J. L. Pearce, B. Powers, C. Hess, P. E. Rybski, S. A. Stoeter, and N. Papanikolopoulos, "Using virtual pheromones and cameras for dispersing a team of multiple miniature robots," *Journal of Intelligent and Robotic Systems*, vol. 45, no. 4, pp. 307–321, Apr. 2006.
- [11] G. Silva, J. Costa, T. Magalhaes, and L. Reis, "CyberRescue: a pheromone approach to multi-agent rescue simulations," in *2010 5th Iberian Conference on Information Systems and Technologies (CISTI)*, Jun. 2010, pp. 1–6.
- [12] C. Skjetne, P. C. Haddow, A. Rye, H. a. Schei, and J.-M. Montanier, "The ChIRP robot: A versatile swarm robot platform," in *Robot Intelligence Technology and Applications 2*. Springer International Publishing, 2014, pp. 71–82.
- [13] N. Bredeche, J.-M. Montanier, B. Weel, and E. Haasdijk, "Roborobo! a fast robot simulator for swarm and collective robotics," *CoRR*, vol. abs/1304.2888, 2013.
- [14] R. A. Brooks, "A robust layered control system for a mobile robot," *Robotics and Automation, IEEE Journal of*, vol. 2, no. 1, pp. 14–23, 1986.
- [15] D. Floreano and C. Mattiussi, *Bio-Inspired Artificial Intelligence: Theories, Methods, and Technologies*, ser. Intelligent robotics and autonomous agents. MIT Press, 2008.
- [16] M. Barthlemy and A. Flammini, "Modeling urban street patterns," *Physical review letters*, vol. 100, no. 13, p. 138702, 2008.